Chapter 17

Subcritical Water Extraction

A. Haghighi Asl and M. Khajenoori

Additional information is available at the end of the chapter

http://dx.doi.org/10.5772/54993

1. Introduction

Extraction always involves a chemical mass transfer from one phase to another. The principles of extraction are used to advantage in everyday life, for example in making juices, coffee and others. To reduce the use of organic solvent and improve the extraction methods of constituents of plant materials, new methods such as microwave assisted extraction (MAE), supercritical fluid extraction (SFE), accelerated solvent extraction (ASE) or pressurized liquid extraction (PLE) and subcritical water extraction (SWE), also called superheated water extraction or pressurized hot water extraction (PHWE), have been introduced [1-3].

SWE is a new and powerful technique at temperatures between 100 and 374°C and pressure high enough to maintain the liquid state (Fig.1) [4]. Unique properties of water are namely its disproportionately high boiling point for its mass, a high dielectric constant and high polarity [4]. As the temperature rises, there is a marked and systematic decrease in permittivity, an increase in the diffusion rate and a decrease in the viscosity and surface tension. In consequence, more polar target materials with high solubility in water at ambient conditions are extracted most efficiently at lower temperatures, whereas moderately polar and non-polar targets require a less polar medium induced by elevated temperature [5].

Based on the research works published in the recent years, it has been shown that the SWE is cleaner, faster and cheaper than the conventional extraction methods. The essential oil of *Z. multiflora* was extracted by SWE and compared with two conventional methods, including hydrodistillation and Soxhlet extraction [7]. The total extraction yields found for the total essential oil of *Z. multiflora* were 2.58, 1.51 and 2.21% (w/w) based on the dry weight for SWE, hydrodistillation and Soxhlet extraction, respectively.

The comparison among the amount of thymol and carvacrol (milligram per gram dried sample) by SWE, hydrodistillation and Soxhlet extraction is shown in Table 1 [7]. The amount of valuable oxygenated components in the SWE method is significantly higher than hydro-

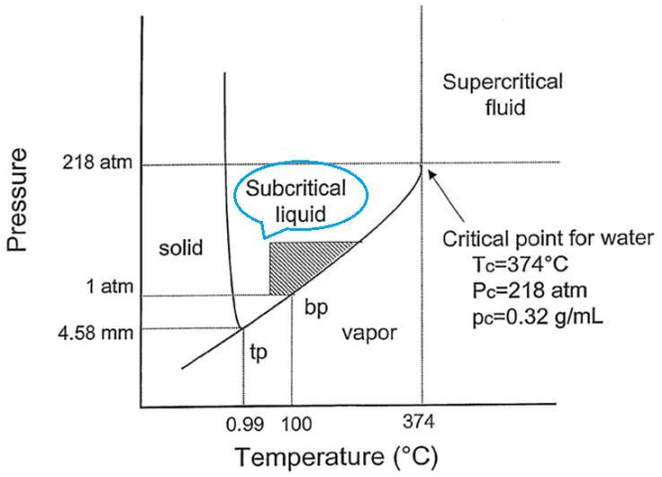

Figure 1. Phase diagram of water as a function of temperature and pressure (Cross-hatched area indicates the preferred region (SWE)) [4].

Components	SWE*	Hydrodistillation†	Soxhlet extraction‡	RI§
Thymol	9.25 (4.77%)**	4.38 (2.97%)	0.94 (2.78%)	1,232
Carvacrol	11.51 (4.33%)	4.06 (3.31%)	1.39 (2.83%)	1,242

Sample weight = 4 g; particle size = 0.5 mm; flow rate = 2 mL/min; temperature = 150C; pressure = 20 bar; and extraction time = 150 min.

* Extraction time = 150 min.

** Relative SD percent.

† Extraction time = 180 min.

‡ Extraction time = 210 min.

§ Retention indices (RI) on the DB-5 column.

* Extraction time = 150 min.

** Relative SD percent.

1' Extraction time = 180 min.

i Extraction time = 210 min.

§ Retention indices (RI) on the DB-5 column.

Table 1. The amount of Thymol and carvacrol (mg/g dried sample) of the essential oil of *Z.multiflora*, extracted by SWE, hydrodistillation and Soxhlet extraction [7].

distillation and Soxhlet extraction. As hexane is a nonpolar solvent, non-oxygenated components are enhanced compared to subcritical water. On the other hand, in general, non-oxygenated components present lower vapor pressures compared to oxygenated components, and in this sense, its content in hydrodistillated extracts are increased. Because of the significant presence of the oxygenated components, the final extract using the SWE method was relatively better and more valuable.

http://dx.doi.org/10.5772/54993

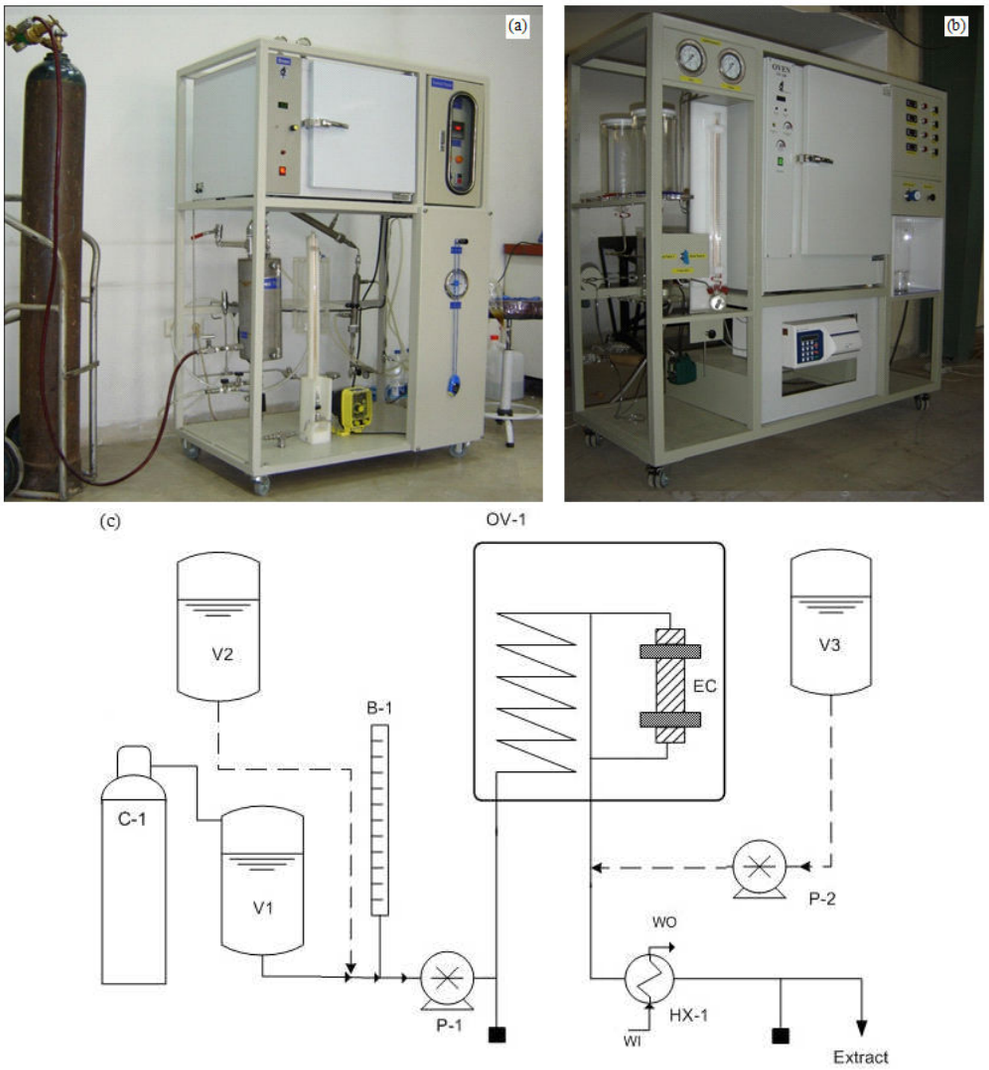

Figure 2. (a) and (b) pictures of first and second generated systems respectively and (c) Schematic diagram of SWE system, B-1: Burette, C-1: Nitrogen cylinder, EC: Extraction cell, HX-1: Heat Exchanger, OV-1: Oven, P-1, 2: Pumps, V-1: Water tank, V-2: Solvent tank, V-3: Rinsing solvent tank, WI: Water inlet, WO: Water outlet.

2. Equipment of subcritical water extraction

No commercial SWE equipment is available, but the apparatus is easy to construct in the laboratory. SWE is performed in batch or continue systems but continue system is current. In this system, extraction bed is fixed and flow direction is usually up to down for easily cleaning of analytes. Already, we worked SWE of *Z. multiflora* with first generated system (Iranian Research Organization for Science and Technology [IROST], Tehran, Iran) [7] (Fig. 2(a)). After it, laboratory-built apparatus of SWE equipment was designed by studying of different systems and have advantages versus first generation (Semnan University, Semnan, Iran) (Fig. 2(b)).

The second generated system is presented in Fig. 2(c). The main parts of a dynamic SWE unit are the following: three tanks, two pumps, extraction vessel, oven for the heating of the

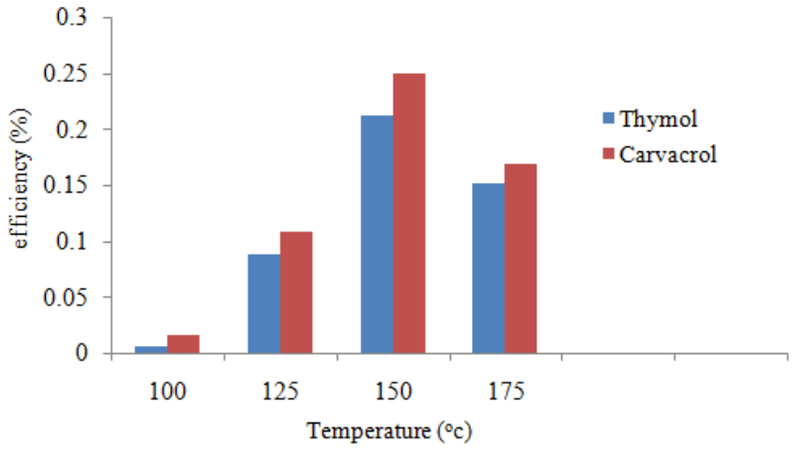

Figure 3. Effect of temperature on the main essential oil components SWE of *Z. multiflora*. Operating conditions: sample weight=4.0 g; flow rate=2 mL/min; particle size=0.50 mm; pressure=20 bar; and extraction time=60 min.

extraction vessel, heat Exchanger for cooling of exteract, pressure restrictor and sample collection system. One of the pumps is employed for pumping the water (and extract) and another pump is employed for flushing the tubings. Also, one of tank is employed for organic solvent that is as a main solvent or co-solvent. A pressure restrictor is needed to maintain the appropriate pressure in the equipment. It was constructed of stainless steel.

3. Effective parameters in subcritical water extraction

3.1. Effect of temperature

One of the most important parameters affecting SWE efficiencies is the extraction temperature. As the temperature rises, there is a marked and systematic decrease in permittivity, an increase in the diffusion rate and a decrease in the viscosity and surface tension. SWE must be carried out at the highest permitted temperature. It should be mentioned that increasing the extraction temperature above a certain value gives rise to the degradation of the essential oil components. The maximum permitted extraction temperature must be obtained experimentally for different plant materials. Regarding the extraction of essential oils, it has been shown that temperatures between 125 and 175°C will be the best condition. The extraction temperature for *Z. multiflora* was optimized in order to maximize the efficiency of thymol and carvacrol (structural isomers) as key components (more than 72%) [7]. Its influence was studied between 100 and 175°C, and the mean particle size, flow rate, extraction time and pressure were selected to be 0.5 mm, 2 ml/min, 60 min and 20 bar pressure, respectively (Fig. 3).

It was seen that the efficiency of thymol and carvacrol increased generally with increase in temperature up to 150°C. At 175°C, it decreased, and an extract with a burning smell was produced. It may be the result of degradation of some of the constituents at higher temperatures. Because of the highest efficiency of thymol and carvacrol essential oil at 150°C and the

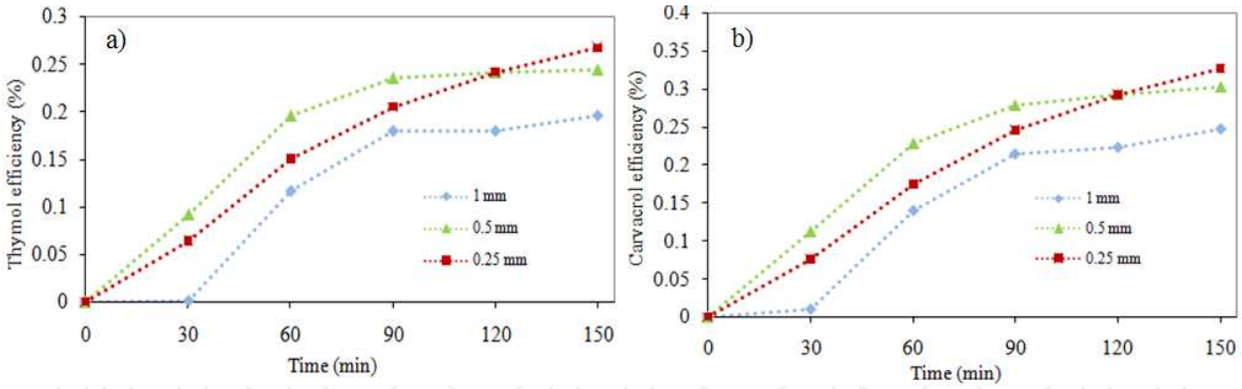

Figure 4. Effect of particle size on the efficiency of a) thymol and b) carvacrol SWE of *Z.multiflora.* Operating conditions: sample weight = 4.0g; flow rate = 2 ml/min; temperature = 150°C; and pressure = 20 bar [7].

disagreeable odor of the extract at higher temperatures, further experiments were carried out at this temperature.

3.2. Effect of particle size

The effect of the mean particle size on the efficiency of thymol and carvacrol at 150°C temperature, 2ml/min flow rate, 20 bar pressure and 150 min extraction time is shown in Fig. 4 [7]. The mean ground leaf particles were selected to be 0.25, 0.5 and 1.0 mm. The final amount of thymol and carvacrol extracted from 0.5-mm-size particles was near to 0.25-mm particles. It shows that, at least in the selected range of mean particle sizes (0.25-0.5 mm), the extraction process may not be controlled by the mass transfer of thymol and carvacrol. It was expected that the rate of the 0.25-mm-size particles was more than the 0.5-mm-size particles, but it did not happen.

A possible explanation for this observation could be that the particles were close fitting at initial times, and the extraction was done slowly. After the expired time, the close fitting particles opened from each other, and at final extraction value of the 0.25-mm-size particles was more than the 0.5-mm-size particles. Regarding the larger 1.0-mm-size particles, the efficiency is substantially lower. It shows that the process may be controlled by the mass transfer of thymol and carvacrol for larger particle sizes.

To prevent the probable vaporization of the essential oils during the grinding of the leaves and also to make the work of the filters easier, for further experiments, the best value of mean particle size was selected as 0.50 mm.

3.3. Effect of flow rate

The effect of water flow rate on the efficiency of thymol and carvacrol at 150°C temperature, 0.5-mm-particle size, 20 bar pressure and 150 min extraction time is shown in Fig. 5 [7]. The water flow rate was studied at 1, 2 and 4 ml/min. As can be seen, the rate of the essential oil extraction was faster at the higher flow rate. The rate is slower at 2 ml/min and even slower at 1 ml/min. It is in accordance with previous works [8, 9]. It means that the mass transfer of the

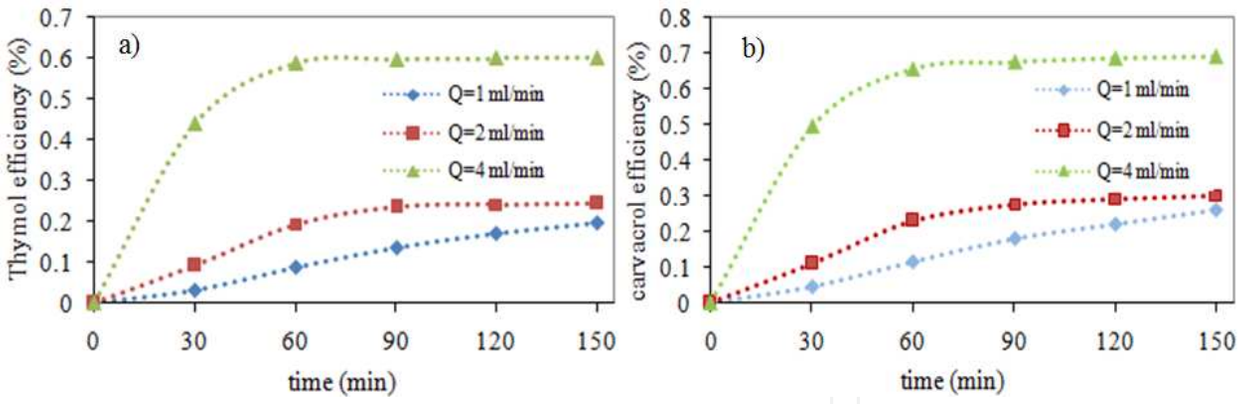

Figure 5. Effect of flow rate on the efficiency of a) thymol and b) carvacrol SWE of *Z. multiflora.* Operating conditions: sample weight = 4.0g; particle size= 0.5 mm; temperature = 150°C; and pressure = 20 bar [7].

thymol and carvacrol components from the surface of the solid phase into the water phase regulated most of the extraction process. Increase in flow rate resulted in increase in superficial velocity, and thus, quicker mass transfer [10]. The main disadvantage of applying higher water flow rates is increasing the extract volume and consequently, lower concentration of the final extracts. In practice, the best flow rate must be selected considering two important factors, including the extraction time and the final extract concentration. It is clear that a shorter extraction time and more concentrated extracts are desirable. To prevent a slower extraction rate and longer extraction times, despite the larger amount of the final extracts, a flow rate of 2 ml/min was selected as the optimum value.

While temperature, particle size and flow rate extraction are the main parameters affecting SWE, type of analyte, extraction vessel characteristics and use of modifiers and additives are also important. Although matrix and other effects play a role, many of these are less critical in SWE than in SFE because of the harsh extraction conditions (high temperature) typical in SWE, particularly for non-polar analytes.

4. Extraction mechanism

The SWE process can be proposed to have six sequential steps: (1) rapid fluid entry; (2) desorption of solutes from matrix active sites; (3) diffusion of solutes through organic materials; (4) diffusion of solutes through static fluid in porous materials; (5) diffusion of solutes through layer of stagnant fluid outside particles; and (6) elution of solutes by the flowing bulk of fluid (Fig. 6).

As we know, the extraction rate is limited by the slowest of these three steps. The effect of step (1) is typically small and often neglected. Although the diffusion of the dissolved solute within the solid is usually the rate limiting step for most botanicals, partitioning of solute between the solid matrix and solvent have been reported as the rate-limiting mechanism for SWE of essential oil from savory [10].

http://dx.doi.org/10.5772/54993

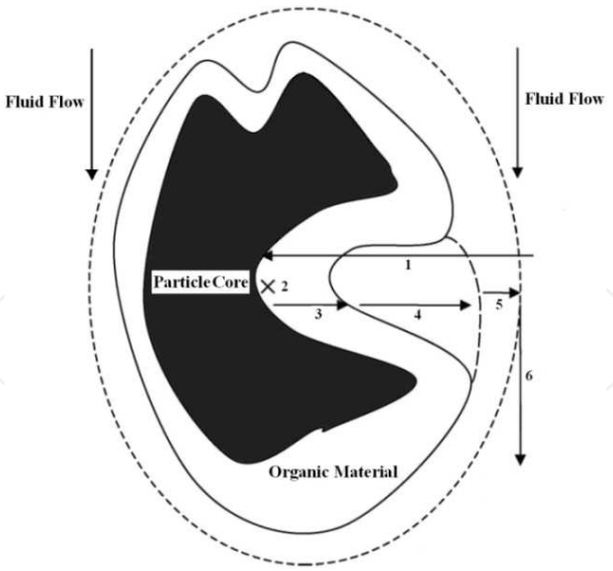

Figure 6. Proposed schematic presentation of the extraction steps in SWE.

The plots the amount of compound extracted versus solvent flow rates and versus solvent volume can determine the relative importance of these steps. For example, if the rate of extraction is controlled by intra-particle diffusion or kinetic desorption, the increase in bulk fluid flow rate would have little effect on extraction rate. On the other hand, if the extraction is controlled by external film transfer diffusion, extraction rates increase with solvent flow rate. In the case where the extraction rate is controlled by thermodynamic partitioning, doubling the bulk fluid flow rate would double the extraction rate, while the curves of extraction efficiency versus the volume of water passed for all flow rates would overlap. In one of our previous work, four proposed models have been applied to describe the extraction mechanisms obtained with SWE of *Z. multiflora* essential oil. These were included (1) partitioning coefficient model, (2) one-site (3) two-site desorption models and (4) thermodynamic partition with external mass transfer model [11]. In other studying unsteady state mass balance of the solute in solid and subcritical water phases (two-phase model) was investigated [12]. Also Computational Fluid Dynamics (CFD) modeling of extraction was considered [13].

5. Modeling of SWE

5.1. Thermodynamic model (Partitioning coefficient (K_D) model)

Partitioning coefficient model, adopted from Kubatova et al. [10], describes the extraction process that is controlled by partitioning of solute between matrix and solvent similar to elution of solute from a partition chromatography column. For extraction, this type of behavior occurs when the initial solute concentration in the plant matrix is small. This model assumes that the initial desorption step and the subsequent fluid-matrix partitioning is rapid. Here the thermodynamics partitioning coefficient, K_D, is defined as:

$$K_D = \frac{Concentration\ of\ \ solute\ in\ the\ matrix}{Concentration\ of\ \ solute\ in\ the\ extraction\ \ fluid}\ ;at\ \ equilibrium \tag{1}$$

Hence the Extraction with subcritical water can be fitted using this simple thermodynamic model. The mass of analyte in each unit mass of extraction fluid and the mass of analyte remaining in the matrix at that period in the entire extraction time is based on the K_D value determined for each compound. The thermodynamic elution of analytes from matrix was the prevailing mechanism in SWE as evidenced by the fact that extraction rate increased proportionally with the subcritical water flow rate. Therefore, if the K_D model applies to a certain extraction, the shape of an extraction curve would be defined by:

$$\frac{M_b}{M_i} = \frac{\left(1 - \frac{M_a}{M_i}\right)}{\left(\frac{K_D m}{(V_b - V_a)\rho} + 1\right)} + \frac{M_a}{M_i} \tag{2}$$

M_a: cumulative mass of the analyte extracted after certain amount of volume V_a (mg/g dry sample)

M_b: cumulative mass of the analyte extracted after certain amount of volume V_b (mg/g dry sample)

M_i: total initial mass of analyte in the matrix (mg/g dry sample)

M_b/M_i and M_a/M_i: cumulative fraction of the analyte extracted by the fluid of the volume V_b and V_a (ml)

K_D: distribution coefficient; concentration in matrix/concentration in fluid

ϱ: density of extraction fluid at given condition (mg/ml)

e: exponential function

m: mass of the extracted sample (mg dry sample).

The model eq. (1) and the experimental data for *Z. multiflora* from all volumetric flow rate, were used to determine the K_D value by minimizing the errors between the measured data and the K_D model using Matlab curve fitting solver. The values of K_D are shown in Table 2 for different flow rates [11]. It was demonstrated that individual essential oil compounds have a range of K_D values from ~4 to ~250 [10].

Flow rate/ ml·min^{-1}	K_D	
	Thymol	Carvacrol
1	80	70
2	80	70
4	2	2

Table 2. K_D values of partitioning coefficient model for different volumetric flow rates [11].

http://dx.doi.org/10.5772/54993

5.2. Mass transfer models

5.2.1. Diffusion model

Mass transfer can be defined as the migration of a substance through a mixture under the influence of a concentration gradient in order to reach chemical equilibrium. The diffusion coefficient (D_e) is the main parameter in Fick's law, and application of this mathematical model to solid foods during solid-liquid extraction is a common way to calculate the effective diffusion coefficient (Crank, 1975 [14]). However, Gekas (1992) noted, values of D_e can vary by several orders of magnitude for the same material which may be due to structural changes in the food material during different stages of the process [15]. Therefore, it is important to keep a constant particle size as breakage of cell wall or grinding can reduce the particle size and hence decrease the distance for solute to travel from inside to surface of particle.

Fick derived a general conservation equation for one-dimensional non-steady state diffusion when the concentration within the diffusion volume changes with respect to time, known as Fick's second law (Cussler, 1984; Mantell et al., 2002) [16, 17]:

$$\frac{\partial C}{\partial t} = D_e \frac{\partial^2 C}{\partial r^2}$$

With the initial condition:

$$C_{(t=0)} = C_o \qquad \text{a}$$

And boundary conditions:

$$\frac{\partial C}{\partial r}_{(r=0)} = 0 \qquad \text{b}$$

$$C_{(r=R)} = 0 \qquad \text{c} \tag{3}$$

Where C is the solute concentration (mg/ml) at any location in the particle at time t (s); C_o is the initial solute concentration (mg/ml); D_e is the effective diffusion coefficient (m^2/s) assuming that D_e is constant with the concentration; t is extraction time (s); r is the radial distance from the centre of a spherical particle (m); R is radius of spherical particle (m).

Various solutions of Fick's second law have been presented for the diffusion of a compound during solid-liquid extraction depending on the shape of the particle. An approximate numerical solution to Fick's second law (eq. 2) for a spherical particle was given by Crank (1975) and Cussler (1984):

$$\frac{M_t}{M_\infty} = 1 - \frac{6}{\pi^2} \sum_{n=1}^{\infty} \frac{1}{n^2} \exp\left[\frac{-D_e n^2 \pi^2 t}{R^2}\right] \tag{4}$$

Where M_t: total amount of solute (mg/g) removed from particle after time t, M_∞: maximum amount (mg/g) of solute extracted after infinite time. M_t/M_∞: ratio of total migration to the

maximum migration concentration, R: average radius of an extractable particle. When time becomes large, the limiting form of Eq. 3 becomes:

$$1 - \frac{M_t}{M_\infty} = \frac{6}{\pi^2} \exp\left[\frac{-D_e \pi^2 t}{R^2}\right] \tag{5}$$

To determine the effective diffusion coefficient values two methods were used. The first method was a linear (graphical) solution in which D_e was determined from the slope of the ln ($1-M_t/M_\infty$) vs. time plot (Dibert et al., 1989) [18]. Thus, eq. 4 can be solved by taking the natural logarithm of both sides. It shows that the time to reach a given solute content will be directly proportional to the square of the particle radius and inversely proportional to D_e:

$$ln\left[1 - \frac{M_t}{M_\infty}\right] = \ln\frac{6}{\pi^2} - \frac{-D_e \pi^2 t}{R^2} \tag{6}$$

Where slope $= \frac{\pi^2 D_e}{R^2}$.

The second method of solution used involved nonlinear regression with effective diffusivity (D_e) as a fitting parameter. In this method, the effective diffusivity D_e was estimated from eq. 4 using a Microsoft Excel Solver program. The program minimizes the mean square of deviations between the experimental and predicted ln($1-M_t/M_\infty$) values (Tutuncu and Labuza, 1996) [19]. The first 10 terms of the series solution are taken into consideration by the program as the solution to the series becomes stable after 10 terms (n=10).

Most researchers in this area have adopted diffusion models based on solutions to Fick's second law for various defined geometrical shapes of the solid given in Crank method, usually based on infinite or semi-infinite geometries of a slab (plane sheet), a cylinder or a sphere. For example, a slab can be used to describe an apple slice or a sheet of herring muscle; a sphere for the description of coffee beans or particles of cheese curd, and a cylinder for the description of cucumber pickles. There is considerable variation in the solutions adopted by various researchers. The starting point for modeling a particular diffusion process is to consider the shape of the solid and the nature of the process itself: uptake of solute into the food, leaching of solute from the food or diffusion of solute through the food, and the experimental conditions in terms of initial and equilibrium solute concentrations.

The solution models usually consider a uniform initial solute concentration throughout the food, no resistance to mass transfer in the diffusion medium and no chemical reaction; but vary for a particular geometry depending on the solute concentrations at the surface of the solid, the volume of the solution (and therefore the relative change in solute concentration in the external solvent), and the time period of the experiment. A representative selection of solutions is given in Table 3. For example, Bressan et al. investigated solute diffusional loss from coffee beans and cottage cheese curd, respectively [20]; they chose solution models to Fick's second law from Crank which assumed the geometry of the solids approximate to that of infinite spheres. However, the former researchers considered a system in which the solute

concentration in the external solvent remains effectively constant and zero throughout the extraction. This can be the case for large infinite solvent volumes and small solute solid concentrations. The latter group of researchers considered a process where the concentration of the solute in the surrounding medium changes significantly. This can be the case for small solvent volumes and high solid phase solute concentrations in the case of leaching, and high external solvent concentrations in the case of solute uptake processes; and consequently adopted a different model.

5.2.2. One-site kinetic desorption model

One-site kinetic desorption model describes the extractions that are controlled by intra-particle diffusion. This occurs when the flow of fluid is fast enough for the concentration of a particular solute to be well below its thermodynamically controlled limit. The one-site kinetic model was derived based on the mass transfer model that is analogous to the hot ball heat transfer model [29, 30]. The assumptions are that the compound is initially uniformly distributed within the matrix and that, as soon as extraction begins, the concentration of compound at the matrix surfaces is zero (corresponding to no solubility limitation). For a spherical matrix of uniform size, the solution for the ratio of the mass, M_r, of the compound that remains in the matrix sphere after extraction time, t, to that of the initial mass of extractable compound, M_i is given as:

$$\frac{M_r}{M_i} = \frac{6}{\pi^2}\sum_{n=1}^{\infty}\frac{1}{n^2}\exp(-D_e n^2\pi^2 t / r^2) \tag{7}$$

In which n is an integer and D_e is the effective diffusion coefficient of the compound in the material of the sphere (m^2/s).

Diffusion process	Diffusion equation	Experimental measurements	**Calculation Diffusivity**
proteins Diffusion though a potato disk [21]	$M_t = \frac{S D_e C_{L\ 1} t}{a} + \frac{2aS}{\pi^2} =$ $1 - \sum_{n=1}^{\infty}\left(C_{L\ 1}\cos(n\pi)exp\left[\frac{-D_e n^2 t}{a^2}\right]\right)$	Protein concentration on the source side initially; at intervals on receiving side	Fitting the experimental values for M_t to the equation by non-linear regression
Analytes diffusion though an apple disk [22]	$M_t = \frac{XAD_e(C - C_L)}{2a}$ A simple lumped parameter equation model	soluble analytes content in the limited volume of solvent	A single effective diffusivity was calculated for each set of data directly from the formula
Analytes diffusion though cheese curd [19]	$\frac{M_t}{M_\infty} = 1 - \sum_{n=1}^{\infty}\frac{6a(1+a)}{9 + 9a + q_n^2 a^2}exp\frac{-D_e q_n^2 t}{2a}$:	Samples of solvent surrounding curd	Experimental data fitted to the equation model

Diffusion process	Diffusion equation	Experimental measurements	**Calculation Diffusivity**
	Solution of Fick's 2nd law for solute loss or uptake for sphere geometry but for finite volume of solvent with attainment of equilibrium	withdrawn at intervals	
Analytes diffusion though carrot cylinders [23]	$E = \frac{C - C_L}{C_i - C_L} =$ $1 - \frac{4}{\pi^{\frac{1}{2}}}\left(\frac{D_e t}{a^2}\right)^{1/2} - \frac{D_e t}{a^2} - \frac{1}{3\pi^{\frac{1}{2}}}\left(\frac{D_e t}{a^2}\right)^{3/2}$: Solution of Fick's 2nd law for solute loss or uptake for an infinite cylinder for short time periods. Authors then modify values to apply to finite cylinder	Carrot samples withdrawn for analysis at intervals	Dimensionless time values calculated for each data point using equation, linear regression of Fourier relationship yields D_e
Analytes diffusion though potato tissue [24]	$\frac{M_t}{M_i} = \frac{8}{\pi^2}\sum_{n=0}^{\infty}\frac{1}{(2n+1)^2} exp\frac{-D_e(2n+1)^2}{a^2}\pi^2 t$: Solution of Fick's 2nd law similar to flow through a membrane	Samples of solvent surrounding slices withdrawn and assayed at intervals, material balance used to calculate M_i and M_t	Equation model modified by omitting terms n"/>0 and natural logarithms, by non-linear regression of $ln\ M_i/M_t$ against t
Analytes and pectic substances diffusion though apple tissue [25]	$E = \frac{C - C_L}{C_i - C_L} = \frac{M_t}{M_i} =$ $\frac{8}{\pi^2}\sum_{n=0}^{\infty}\frac{1}{(2n+1)^2} exp\left[-(2n+1)^2\left(\frac{D_e t}{a^2}\right)\frac{\pi^2}{2}\right]$: Solution of Fick's 2nd law for diffusion from an infinite slab developed by Newman [59]	Apple slices withdrawn for analysis at intervals	A series of dimensionless time values found for data using Newman's tables. D_e calculated by linear regression of Fourier relationship
Analytes diffusion though apple tissue [26]	$E = \frac{M_t}{M_i} = \frac{512}{\pi^6} exp\left[-\frac{\pi^2 D_e}{4(a^2 + b^2 + c^2)}\right]t$: Equation model adopted considers diffusion in a slab in three planes.	Apple slices withdrawn for analysis at intervals	Modification of equation model by natural logarithms enables regression of lnE against t give slope with D_e term
Salt and acetic acid diffusion though herring [27]	$\frac{M_t}{M_\infty} = 1 - \sum_{n=0}^{\infty}\frac{8}{(2n+1)^2\pi^2} exp\left[\frac{-D_e(2n+1)^2\pi^2 t}{4a^2}\right]$: Solution of Fick's 2nd law for diffusion from/or uptake by infinite solution.	Fish withdrawn for analysis at intervals	Experimental data fitted to equation model by successive approximations
Analytes diffusion though potato tissue [28]	$\frac{M_t}{M_\infty} = \frac{V_L\ C_{Li} - V_L\ C_L}{V_L\ C_{Li} - V_L\ C_\infty} =$ $1 - \sum_{n=1}^{\infty}\frac{2\alpha(1+\alpha)}{1 + \alpha + \alpha^2 n^2} exp\frac{-D_e n^2 t}{a^2}$:	Initial solute content of potato strip and solute contents of solvent	Minimizing the residuals between experimental data and theoretical

Diffusion process	Diffusion equation	Experimental measurements	**Calculation Diffusivity**
	Solution of Fick's 2nd law for diffusion from/or uptake by an infinite slab for uptake from a solution of finite volume. $\frac{M_t}{M_\infty} = 1 - \sum_{n=0}^{\infty} \frac{8}{(2n+1)^2\pi^2} exp\left[\frac{-D_e(2n+1)^2\pi^2 t}{4a^2}\right]$: Solution of Fick's 2nd law for diffusion from/or uptake by infinite slab.	surrounding strip at intervals	values for M_t/M_∞ obtained from the appropriate equation models

Table 3. Diffusion phenomena.

The curve for the above solution tends to become linear at longer times (generally after t > 0.5 t_c), and ln (M_r/M_i) is given approximately by:

$$Ln(M_r / M_i) = -0.4977 - t / t_0 \tag{8}$$

Where t_c (min) is a characteristic time quantity, defined as:

$$t_c = r^2 / \pi^2 D_e \tag{9}$$

An alternative form of eq. 7, or so called a one-site kinetic desorption model, can be written for the ratio of mass of analyte removed after time *t* to the initial mass, M_i, as given by:

$$\frac{M_t}{M_i} = 1 - e^{-kt} \tag{10}$$

In which M_t is the mass of the analyte removed by the extraction fluid after time t (mg/g dry sample), M_i is the total initial mass of analyte in the matrix (mg/g dry sample), M_t/M_i is the fraction of the solute extracted after time t, and k is a first order rate constant describing the extraction (min^{-1}).

Matlab curve fitting solver was used to determine the desorption rate constant, k, from the data for all flow rates. The values for *Z. multiflora* SWE are show in Table 4 [11]. As mentioned, the kinetic desorption model does not include a factor describing extraction flow rate, k should be the same value for all flow rates if the model is said to fit the experimental data. However, this was not the case (Table 4, the average error 3%-17%). The kinetic desorption rate increased for the volumetric flow rate of 1 to 4 ml/min. This indicated that the kinetic desorption model may not be suitable for describing the data at different flow rates of *Z. multiflora*.

5.2.3. Two-site kinetic desorption model

Two-site kinetic model is a simple modification of the one-site kinetic desorption model that describes extraction which occurs from the "fast" and "slow" part [10]. In such case, a certain

Flow rate/ ml·min^{-1}	k/min^{-1}	
	Thymol	Carvacrol
1	0.0025	0.0028
2	0.0042	0.0039
4	0.0157	0.0157

Table 4. Values of k for one-site kinetic desorption model for different volumetric flow rates [7].

fraction (F) of the analyte desorbs at a fast rate defined by k_1, and the remaining fraction (1-F) desorbs at a slower rate defined by k_2. The model has the following form:

$$\frac{M_t}{M_i} = 1 - \left[Fe^{-k_1 t} \right] - \left[(1-F)e^{-k_2 t} \right] \tag{11}$$

The two site kinetic model does not include solvent volume, but relies solely on extraction time. Therefore, doubling the extractant flow rate should have little effect on the extraction efficiency when plotted as a function of time. On the contrary, the thermodynamic model is only dependent on the volume of extractant used. Therefore, the extraction rate can be varied by changing the flow rate. Hence, the mechanism of thermodynamic elution and diffusion kinetics can be compared simply by changing the flow rate in SWE. If the concentration of bioactive compounds in the extract increases proportionally with an increase in flow rate at given extraction time when the solute concentration is plotted versus extraction time, the extraction mechanism can be explained by the thermodynamic model. However, if an increase in flow rate has no significant effect on the extraction of the bioactive compounds, with the other extraction parameters being kept constant, the extraction mechanism can be modeled by the two site kinetic model [10, 31]. The mechanism of control and hence the model valid for SWE may be different depending on the raw material, the target analyte and extraction conditions.

For the two-site kinetic desorption model, the values of k_1 and k_2 were determined by fitting the experimental data with the two-site kinetic desorption models by minimizing the errors between the data and the model results. In the two-site model, the extraction rate should not be dependent on the flow rate. The k_1 and k_2 values for *Z. multiflora* SWE shown in Tables 5 and 6 demonstrated that the extraction rates were not completely independent of flow rate (the average error 11%-20%).

5.2.4. Thermodynamic partition with external mass transfer resistance model

This model describes extraction which is controlled by external mass transfer whose rate is described by resistance type model of the following form:

Flow rate/ml·min^{-1}	k_1/min^{-1}	k_2/min^{-1}	Mole fraction F
1	0.0088	0.0015	0.21
2	0.0152	0.0026	0.28
4	0.0770	0.0083	0.27

Table 5. k_1 and k_2 values of two-site kinetic desorption model for thymol at different flow rates [11].

Flow rate/ml·min^{-1}	k_1/min^{-1}	k_2/min^{-1}	Mole fraction F
1	0.0101	0.0017	0.21
2	0.0747	0.0088	0.42
4	0.0469	0.0082	0.27

Table 6. k_1 and k_2 values of two-site kinetic desorption model for carvacrol at different flow rates [11].

$$\frac{\partial C_s}{\partial t} = -k_e a_p \left[\left(C_s / K_D \right) - C \right] \tag{12}$$

in which C is the fluid phase concentration (mol/m^3), C_s is the solid phase concentration (mol/m^3), k_e is the external mass transfer coefficient (m/min) and a_p is specific surface area of particles (m^2/m^3) [32]. If the concentration of the solute in the bulk fluid is assumed small and the solute concentration in the liquid at the surface of solid matrix is described by partitioning equilibrium, K_D, the solution of eq. 11 for the solute concentration in the solid matrix, C_s, becomes:

$$C_s = C_0 - \exp(-k_e a_p t / K_D) \tag{13}$$

eq. 11 can be rewritten as the ratio of the mass of diffusing solute leaving the sample to the initial mass of solute in the sample, M_t/M_i, as given by the following equation.

$$M_t = 1 - M_i \exp(-k_e a_p t / K_D) \tag{14}$$

Because a_p is difficult to be measured accurately, a_p and k_e are usually determined together as $k_e a_p$, which is called overall volumetric mass transfer coefficient. The factors that influence the value of $k_e a_p$ include the water flow rate through the extractor and the size and shape of plant sample.

The values for the model parameters, K_D and $k_e a_p$ in eq. (9) determined by Matlab curve fitting solver from the experimental data obtained at 150°C are summarized for *Z. multiflora* SWE in

Tables 7 and 8 for different mass flow rates (Q, mg min^{-1}) [11]. Linear regresion of the plot between $\ln(k_e a_p)$ and lnQ gives the following correlation for $k_e a_p$ and Q:

$$\text{for thymol:} \quad k_e a_p = 6.5748\, Q_m^{0.2078} \tag{15}$$

$$\text{for carvacrol:} \quad k_e a_p = 0.1605\, Q_m^{0.6017} \tag{16}$$

Flow rate/ $ml \cdot min^{-1}$	Mass flow rate Q_m/$mg \cdot min^{-1}$	Parameter K_D	Parameter $k_e a_p$/min^{-1}
1	938	80	26.700
2	1876	80	32.7975
4	3752	2	1.300

Table 7. Parameters K_D and $k_e a_p$ for external mass transfer model of SWE of thymol [11].

Flow rate/ $ml \cdot min^{-1}$	Mass flow rate/$mg \cdot min^{-1}$	Parameter K_D	Parameter $k_e a_p$/min^{-1}
1	938	70	8.92
2	1876	70	62.013
4	3752	2	20.54

Table 8. Parameters K_D and $k_e a_p$ for external mass transfer model of SWE of carvacrol [11].

To quantitatively compare the extraction models, the mean percentage errors between the experimental data and the models were considered. Based on the result in fitting from experimental data, the K_D model was generally suitable for the description of extraction over all the volumetric flow rates tested. On the other hand, one-site and two-site kinetic desorption models describe the extraction data reasonably at lower volumetric flow rates. Of all the models considered, however, the thermodynamic partition with external mass transfer model could best describe the experimental data.

5.2.5. Two-phase model

A mathematical model can be developed to predict optimal operating parameters for SWE in a packed-bed extractor. Three important steps consist of diffusion of solutes through particles, diffusion and convection of solutes through layer of stagnant fluid outside particles and elution of solutes by the flowing bulk of fluid are assumed. Unsteady state mass balance of the solute in solid and subcritical water phases led to two partial differential equations. The model can be solved numerically using a linear equilibrium relationship. The model parameters were mass transfer coefficient, axial dispersion coefficient, and intraparticle diffusivity. The last

parameter was selected to be the model tuning parameter. The two other parameters were predicted applying existing experimental correlations.

5.2.5.1. Model description

The more precise method is based on differential mass balances along the extraction bed. A two-phase model comprising solid and subcritical water phases can be used. Extraction vessel is considered to be a cylinder filled by mono-sized spherical solid particles. The overall scheme of system was like Fig. 7.

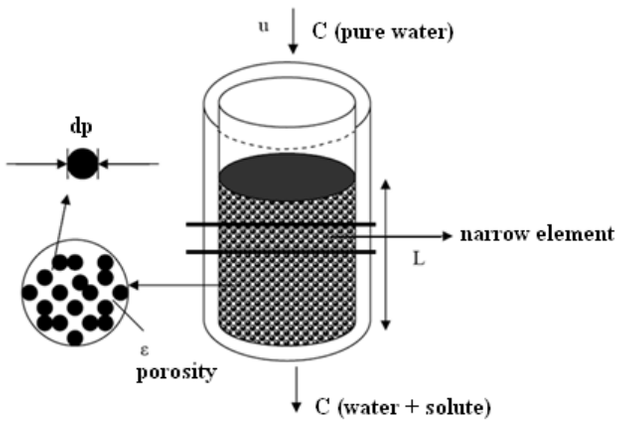

Figure 7. Characteristic dimensions and geometry of the packed bed SWE vessel.

The major assumptions used to describe the SWE process for deriving the essential oils extraction model were:

1. Packed bed extractor was isothermal and isobaric,
2. The physical properties of subcritical water were constant,
3. The hydrodynamics of a fluid bed was described by the dispersed plug-flow model,
4. The radial concentration gradient in the bulk fluid phase was assumed to be negligible,
5. The volume fraction of bed was not influenced by the weight loss of plant during the extraction,
6. The essential oil was assumed as a single component.

Under these assumptions, the differential mass balance equation for any component in the particle and bulk liquid phase and associated initial and boundary conditions can be written as following dimensionless forms:

- Solid phase:

$$\frac{\partial C_p}{\partial \tau} = \frac{2}{Pe_p}\frac{L}{R}\left(\frac{\partial^2 C_p}{\partial Y^2} + \frac{2}{Y}\frac{\partial C_p}{\partial Y}\right) \tag{17}$$

$$\tau = 0 \qquad C_p = C_{p0} \tag{18}$$

$$Y = 0 \qquad \frac{\partial C_p}{\partial Y} = 0 \tag{19}$$

$$Y = 1 \quad \frac{\partial C_p}{\partial Y} = Sh\left(C_f - C_{fp}\right) \tag{20}$$

- Subcritical water phase

$$\frac{\partial C_f}{\partial \tau} = \frac{1}{Pe_b}\frac{\partial^2 C_f}{\partial X^2} - \frac{\partial C_f}{\partial X} - \frac{6(1-\varepsilon)L}{\varepsilon R}\frac{Bi}{Pe_p}\left(C_f - C_{fp}\right) \tag{21}$$

$$\tau = 0 \qquad C_f = 0 \tag{22}$$

$$X = 0 \qquad C_f - \frac{1}{Pe_b}\frac{\partial C_f}{\partial X} = 0 \tag{23}$$

$$X = 1 \quad \frac{\partial C_f}{\partial X} = 0 \tag{24}$$

Eqs. (17) and (21) may be solved using a linear equilibrium relationship between concentrations in the solid phase and SW phase at the interface, as follows [33]:

$$C_{fp} = k_p C_p\big|_{Y=1} \tag{25}$$

Where C_{fp} is the solute concentration in the fluid phase at the particle surface, $C_p|_{Y=1}$ is the solute concentration in the solid phase at equilibrium with the fluid phase and k_p is the volumetric partition coefficient of the solute between the solid and the fluid phase. Therefore, there are three eqs. (17), (21) and (25) which can be solved, simultaneously, for three unknowns C_p, C_f and C_{fp}.

The finite difference equations are a set of simultaneous linear algebraic equations must be solved for implicit method to obtain the concentration distribution at any time. In both cases, tridiagonal systems arise which are conveniently solved at each time step by the Thomas algorithm [34]. A computer code was written using MATLAB simulation software.

5.2.5.2. Parameter identification and correlations

The possible control of mass transfer was assayed by estimating the diffusion coefficient in the liquid. We can use the correlation proposed by Wilke and Chang (1955) to estimate this coefficient [35]:

$$D_{AB} = \frac{7.4*10^{-8}}{\mu V_A^{0.6}}(\varphi M_2)^{0.5} T \tag{26}$$

Where φ is 2.26 for water and 1.5 for ethanol and V_A was estimated by the Tyn Calus equation:

$$V_A = 0.285\ (V_c)^{1.048} \tag{27}$$

Where V_c is the estimated by the method of Joback and Reid (1987), with the aid of Molecular Modeling Plus software (Norgwyn Montgomery Software, USA) [36]. The axial dispersion coefficient in the supercritical phase was approximated as follows [37] and it may be used for the subcritical phase:

$$D_L = \frac{u\ d_p}{\varepsilon\ Pe_{pd}} \tag{28}$$

Where the average void volume fraction of the fixed bed was ε = 0.4 and:

$$Pe_{pd} = 1.634\ Re^{0.265}\ Sc^{-0.919} \tag{29}$$

Intraparticle diffusivity of the essential oils in the solid phase, D_m, was selected to be the tuning parameter of the model. Mass transfer between liquids and beds of spheres, k_f, can be represented by Wilson and Geankoplis in two cases [38]:

$$\varepsilon\ j_D = 0.0016 < Re < 55, \quad 165 < Sc < 70600 \tag{30}$$

$$\varepsilon\ j_D = \frac{0.25}{Re^{0.31}} 55 < Re < 1500, \quad 165 < Sc < 10690 \tag{31}$$

$$k_f = \frac{J_D\ U_o}{Sc^{2/3}} \tag{32}$$

Density of water at high pressures and temperatures from 273 to 473 K was assumed to be the density of saturated water (kg). It was calculated as follows [39]:

$$\rho = 858.03 + 1.2128\ T - 0.0025\ T^2 \tag{33}$$

Where ϱ is density (kg/m^3) and T is temperature (K). The water viscosity at temperatures from 300 to 450 K was calculated by the following equation:

$$\mu = \exp\left(-10.2 + \frac{280970}{T^2}\right) \tag{34}$$

Where μ is the viscosity (Pa.s) and T is temperature (K). Viscosity of water was supposed to be independent of pressure. The model was verified successfully using the SWE data for *Z.multiflora* leaves at 20 bar and 150°C. The optimum value of 2×10^{-12} m^2/s was obtained for the intraparticle diffusivity [12].

5.2.6. CFD model

There is no scientific literature about the application of CFD modeling approach in the SWE processes. In our previous work, we have tried to do CFD modeling of essential oils of *Z. multiflora* leaves [13].

In CFD modeling in packed bed reactor, there are two cases. In first one, when the reactor to particle diameter ratio is less than10, it is needed to build the exact geometry and the location of the particles and solving the governing equations in meshes and can see the field of flow between particles inside reactor. But in another one, when the reactor to particle diameter ratio is higher than10, this system is defined as porous media. For modeling of these reactors, the Navier-stocks with one additional term, which is contained viscous force and inertia loss, in porous media is solved.

In this work, because of the reactor to particle diameter ratio is higher than10; the system can define as porous media. The momentum equation is defined as:

$$\frac{\partial}{\partial t}\left(\varepsilon\rho\vec{\upsilon}\right)+\nabla.\left(\varepsilon\rho\vec{V}\vec{V}\right)=-\varepsilon\nabla P+\nabla.\left(\varepsilon\tau\right)=\left(-\frac{\mu}{\beta}\vec{V}+\frac{1}{2}C\rho\left|\vec{V}\right|\vec{V}\right) \tag{35}$$

Where $\frac{\partial}{\partial t}(\varepsilon\rho\vec{\upsilon})+\nabla.(\varepsilon\rho\vec{V}\vec{V})=-\varepsilon\nabla P+\nabla.(\varepsilon\tau)=\left(-\frac{\mu}{\beta}\vec{V}+\frac{1}{2}C\rho\mid\vec{V}\mid\vec{V}\right)$ and C and β coefficient can define as:

$$\beta=\frac{d_P^2\varepsilon^3}{150\left(1-\varepsilon\right)^2} \tag{36}$$

$$C=\frac{3.5\left(1-\varepsilon\right)}{d_P\varepsilon^3} \tag{37}$$

In this work the porosity of bed is 0.4, so we have following value for C and β coefficients.

$$C=54687.5\quad 1/m \tag{38}$$

$$\beta=0.23*10^{-10}\,1/m^2 \tag{39}$$

The energy equation is defined as:

$$\frac{\partial}{\partial t}\left(\varepsilon\rho_f E_f+\left(1-\varepsilon\right)\rho_s E_s\right)+\nabla.\left(\vec{V}\left(\rho_f E_f+P\right)\right)=\nabla.\left[\hat{K}\nabla T+\left(\tau.\vec{V}\right)\right]+S \tag{40}$$

http://dx.doi.org/10.5772/54993

Where the Effective thermal diffusion coefficient is defined as:

$$\hat{K} = \varepsilon \hat{K}_f + \left(1-\varepsilon\right)\hat{K}_s \tag{41}$$

The spices transfer equation is defined as:

$$\frac{\partial c_i}{\partial t} + \frac{\partial}{\partial \mathrm{x}}\left(-\mathrm{D}_\mathrm{x}\frac{\partial c_i}{\partial x}\right) + \frac{\partial}{\partial \mathrm{x}}\left(-\mathrm{D}_\mathrm{x}\frac{\partial c_i}{\partial x}\right) = \frac{D_y}{y}\frac{\partial c_i}{\partial y} - \frac{u}{\varepsilon}\frac{\partial c_i}{\partial x} - \frac{u}{\varepsilon}\frac{\partial c_i}{\partial y} + S \tag{42}$$

S is source term. Comparing the default of spices transfer equation with spices transfer equation of this system can define the $\frac{\partial c_i}{\partial t} + \frac{\partial}{\partial \mathrm{x}}\left(-\mathrm{D}_\mathrm{x}\frac{\partial c_i}{\partial x}\right) + \frac{\partial}{\partial \mathrm{x}}\left(-\mathrm{D}_\mathrm{x}\frac{\partial c_i}{\partial x}\right) = \frac{D_y}{y}\frac{\partial c_i}{\partial y} - \frac{u}{\varepsilon}\frac{\partial c_i}{\partial x} - \frac{u}{\varepsilon}\frac{\partial c_i}{\partial y} + S$ as the source term of this work.

C_{fs} was the concentration of Thymol & Carvacrol in the fluid face at the particle surface and was defined as:

$$c_{fs} = k_p c_{ss} \tag{43}$$

and

$$c_{ss} = 0.8\, c_0 \exp\left(-0.0005\, t\right) \tag{44}$$

In such works, the Reynolds number is defined as:

$$\mathrm{Re}_d = \frac{\rho \bar{U}_p \bar{d}_p}{\mu} \tag{45}$$

$\mathrm{Re}_d = \frac{\rho \bar{U}_p \bar{d}_p}{\mu}$ is mean characteristic length of porous and $\bar{d}_p$ is mean velocity based on porous. Based on this Reynolds number, it can be seen four regimes:

Re_d<1 Darcy regime or creeping flow

1<Re_d<150 inertia regime

150<Re_d<300 unsteady laminar flow regime

Re_d>300 unsteady Turbulent flow regime

The superficial velocity in this packed bed is defined as dividing flow rate by cross section.

Dividing superficial velocity by porosity, real velocity can calculate.

$$U = \frac{Q}{A} \tag{46}$$

$$\bar{U}_p = \frac{U}{\varepsilon} \tag{47}$$

and for calculating D_p

$$\bar{D}_p = \frac{6}{A_0} \tag{48}$$

In this work the mean particle diameter was 0.6 mm.

$$A_0 = \frac{A}{V} = \frac{4\pi r^2}{\frac{4}{3}\pi r^3} \tag{49}$$

In this work the Reynolds number is 0.2, so there is laminar flow in this system.

The material of system was mixture of Thymol & Carvacrol and water. The inlet flow was contained water with mole fraction 1 and the outer flow was consisted of water and Thymol & Carvacrol [13]. The packed bed had 103 mm height and the diameter of bed was 16 mm. The uniform mesh was used for this domain.

The governing equations are solved by a finite volume method. At main grid points placed in the center of the control volume, volume fraction, density and spices fraction are stored. The conservation equations are integrated in space and time. This integration is performed using first order upwind differencing in space and fully implicit in time. For a first-order upwind solution, the value at the center of a cell is assumed to be an average throughout the cell. The SIMPLE algorithm is used to relate the velocity and pressure equations.

The simulation geometry is shown in Fig.8. The 2D calculation domain is divided into 22*146 grid nodes, in the radial and axial directions, respectively. The grid and mesh size are chosen to be uniform in the two directions. The inlet of system was pure water and the outlet of system was extracted Thymol & Carvacrol.

The extraction values versus time for 150^{o}C were shown in Fig. 9. It can be seen, the extraction values were increased as exponentially. After 60 min, the change of extraction values with time was very little.

http://dx.doi.org/10.5772/54993

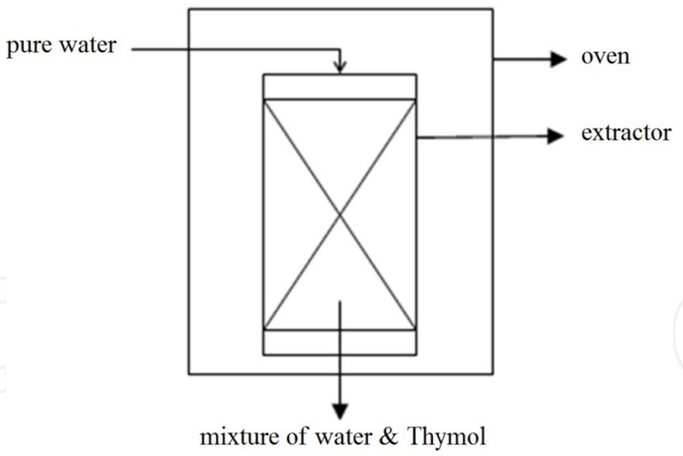

Figure 8. The Schematic of extractor [13].

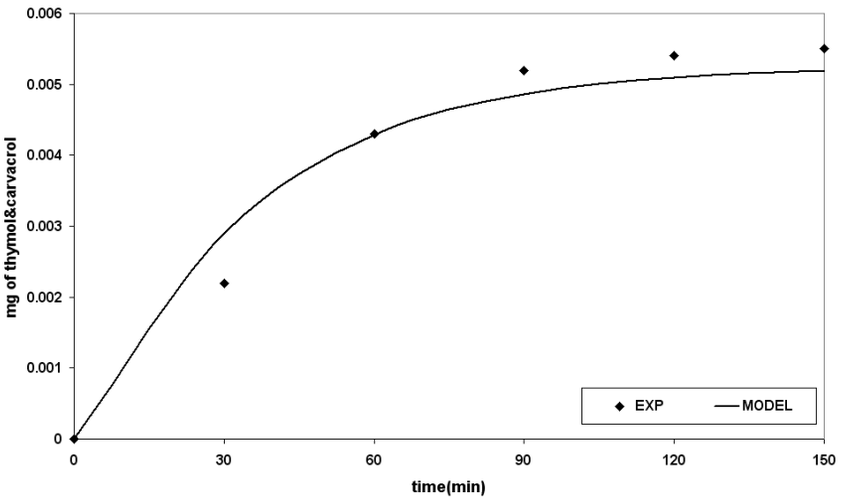

Figure 9. Extraction values versus time for 150°C [13].

In order to investigate the applicability of the CFD model, the theoretical results are compared with experimental measurements obtained at optimum conditions (20 bars, 150°C, and 2 ml/min). Fig. 9 shows that the modeling extraction values profile is increasing rapidly in the period of 0-60 min and thereafter in the second region (60-120 min) the slope reduces until reaches a constant trend in the third period of 120-150 min. In the first region, because of high Thymol & Carvacrol concentrations in the *Z. multiflora* leaves and therefore, high mass transfer driving force, high desorption rate of Thymol & Carvacrol from solid matrix occurs.

6. Conclusion

It was tried to give overall view about subcritical water extraction. Effective parameters, mechanism and modeling of extraction were surveyed. Overall by considering mean average

errors of models, a mathematical model base on the combination of partition coefficient (*K*D) and external mass transfer gave a good description of subcritical water extraction of *Z. multiflora*, while the kinetic model reasonably described the extraction behavior at lower flow rates [11].

On the other side, model was developed by introducing differential mass balances using two phase model, and applying a linear equilibrium relationship. Because of considering the effect of variation of the concentration profile in the SW phase, it seems that the proposed model is more significant from the physical point of view.

The Last model was CFD modeling of extraction from *Z. multiflora* leaves using subcritical water. It was concluded that CFD is poised to remain at the forefront of cutting edge research in the sciences of fluid dynamics and mass transfer. Also, the emergence of CFD as a practical tool in modern engineering practice is steadily attracting much interest and appeal. The results of CFD model have been agreed well with experimental data. As shown, along of extractor, Thymol was extracted and was in outflow.

Notations

specific surface, m^2/m^3 ($=\frac{3}{R_p}$)	a or a_p
Biot number ($=\frac{k_f R_p}{D_m}$)	Bi
solute concentration in the solid phase, $kmol/m^3$	C
solute concentration in the SW phase, $kmol/m^3$	C_f
solute concentration in the fluid phase at the particle surface, $kmol/m^3$	C_{fp}
solute concentration in the solid phase, $kmol/m^3$ ($\frac{C_p}{C_{po}}$)	C_p
initial solute concentration in the solid phase, $kmol/m^3$	C_{po}
diffusivity of solute (A) in liquid (B), m^2/s	D_{AB}
effective diffusion coefficient (m^2/s)	D_e
axial dispersion coefficient, m^2/s	D_L
diffusivity in the solid, m^2/s	D_m
particle diameter, m	d_p
exponential function	e
a certain fraction of the analyte desorbs at a fast rate by k_1	F
remaining fraction desorbs at a slower rate by k_2	$(1-F_1)$
thermodynamics partitioning coefficient	K_D
external mass transfer coefficient (m/min)	k_e

mass transfer between liquids and beds of spheres	k_f
volumetric partition coefficient of the solute between the solid and the fluid phase	k_p
cumulative mass of analyte extracted after certain amount of volume V_a (mg/g dry sample)	M_a
cumulative mass of the analyte extracted after certain amount of volume V_b (mg/g dry sample)	M_b
total initial mass of analyte in the matrix (mg/g dry sample)	M_i
cumulative fraction of the analyte extracted by the fluid of the volume V_b and V_a (ml)	M_b/M_i and M_a/M_i
total amount of solute (mg/g) removed from particle after time t	M_t
maximum amount (mg/g) of solute extracted after infinite time	M_∞
ratio of total migration to the maximum migration concentration	M_t/M_∞
mass of the extracted sample (mg dry sample)	m
Peclet number of the bed (= $\frac{u_o L}{D_L \varepsilon}$)	Pe_b
Peclet number of the solid (= $\frac{u d_p}{D_m \varepsilon}$)	Pe_p
average radius of an extractable particle	R
Reynolds number (= $\frac{2 R u \rho}{\mu}$)	Re
Schmidt number (= $\frac{\mu \rho}{D_{AB}}$)	Sc
Sherwood number (= $\frac{2 kf R}{D_{eff}}$)	Sh
Stanton number ($\frac{L (1 - \varepsilon) k_f a}{u}$)	St
Temperature, K	T
superficial SW fluid velocity, m/s	u
molar volume of the solute at its normal boiling point, cm^3/mol	V_A
critical volume, cm^3/mol	V_c
dimensionless axial coordinate along the bed, z/L	X
dimensionless radius (= $\frac{r}{R}$)	Y

Greek symbols

ε	void volume fraction
μ	viscosity, Pa.s
ρ	density, kg/m^3
φ	association factor for the solvent

τ	dimensionless time ($=\frac{u t}{L \varepsilon}$)

Acknowledgements

This research was supported by Semnan University. The authors would like to thanks the Office of Brilliant Talents at the Semnan University for financial support.

Author details

A. Haghighi Asl and M. Khajenoori

School of Chemical Gas and Petroleum Engineering, Semnan University, Semnan, I.R., Iran

References

[1] C.W. Huie, "A review of modern sample-preparation techniques for the extraction and analysis of medicinal plants," Anal. Bioanal. Chem. 373 (2002) 23-30.

[2] B. Zygmunt, J. Namiesnik, "Preparation of samples of plant material for chromatographic analysis," J. Chromatogr. Sci. 41 (2003) 109-116.

[3] E.S. Ong, "Extraction methods and chemical standardization of botanicals and herbal preparations," J. Chromatogr. B 812 (2004) 23-33.

[4] King, et al., US Patent 7,208,181, B1, 2007.

[5] R. M., Smith, "Superheated water: The ultimate green solvent for separation science", Anal. Bioanal. Chem., 385(3), 419 (2006).

[6] D. J., Miller, S. B., Hawthorne, "Solubility of liquid organics of environmental interest in subcritical (hot/liquid) water from 298 K to 473 K", J. Chem. Eng. Data, 45, 78 (2000).

[7] M. Khajenoori, A. Haghighi Asl, and F. Hormozi, M. H. Eikani and H. Noori. "Subcritical Water Extraction of *Zataria Multiflora Boiss.*", *Journal of Food Process Engineering*, 32, (2009) 804–816.

[8] M.H., Eikani, F., Golmohammad and S., Roshanzamir, "Subcritical water extraction of essential oils from coriander seeds (*Coriandrum sativum Mill.*)", J. Food Eng. 80 (2) (2007a) 735-740.

[9] M.H., Eikani, F., Golmohammad, S., Roshanzamir and M. Mirza, "Extraction of volatile oil from cumin (*Cuminum cyminum L.*) with superheated water", J. Food Process Eng., 30 (2) (2007b) 255-266.

[10] A., Kubatova, B., Jansen, J.F., Vaudoisot, S. B., Hawthorne, "Thermodynamic and kinetic models for the extraction of essential oil from savory and polycyclic aromatic hydrocarbons from soil with hot (subcritical) water and supercritical CO_2", J. Chromatography A., 975(1), (2002) 175-188.

[11] M. Khajenoori, A. Haghighi Asl, and F. Hormozi, "Proposed Models for Subcritical Water Extraction of Essential Oils", Chinese Journal of Chemical Engineering, Vol. 17, No. 3, (2009) 359-365.

[12] M. Khajenoori, A. Haghighi Asl, and M. H. Eikani "Modeling of Superheated Water Extraction of Essential Oils". Submitted in "13th Iranian National Chemical Engineering Congress & 1st International Regional Chemical and Petroleum Engineering Kermanshah, Iran, 25-28 October, 2010".

[13] M. Khajenoori, E. Omidbakhsh, F. Hormozi, and A. Haghighi Asl, "CFD modeling of subcritical water extraction". the 6th International chemical Engineering Congress (IChEC), Kish Island, Iran, 16-20 November 2009.

[14] J., Crank,. "The mathematics of Diffusion". Oxford, England: Clarendon Press. (1975) pp. 150-175.

[15] V., Gekas, "Transport phenomena of foods and biological material". Boca Raton, FL. CRC Press., (1992) pp. 156-178.

[16] E. L., Cussler, "Diffusion: Mass Transfer in Fluid Systems". Cambridge University Press. Cambridge, UK., (1984) pp. 146-177.

[17] C., Mantell, M., Rodriguez, and E. Martinez de la Ossa, "Semi-batch extraction of anthocyanins from red grape pomace in packed beds: experimental results and process modeling", Chem. Eng. Sci., 57 (2002). 3831-3838.

[18] Dibert, K., Cros, E., and Andrieu, J. Solvent extraction of oil and chlorogenic acid from green coffee. Part II. Kinetic data. J. Food Eng., 10, (1989) 199-214.

[19] Tutuncu, M. A., and labuza, T.P.. Effect of geometry on the effective moisture transfer diffusion coefficient. J. Food Eng. 30: (1996) 433-447.

[20] J.A. Bressan, P.A. Carroad, R.L. Merson, W.L. Dunkley, Temperature dependence of effective diffusion coefficient for total solids during washing of cheese curd. J. Food Sci, 46 (1958) 9.

[21] E.S.A., Biekman, C., Van Dijk, "Measurement of the apparent diffusion coefficient of proteins in potato tissue", Presented at DLOA grotechnological Research Institute, The Netherlands, (1992).

[22] C.R., Binkley, RC., Wiley, "Chemical and physical treatment effects on solid–liquid extraction of apple tissue", J. Food Sci., 46 (1981) 729-732.

[23] NS., Kincal, F., Kaymak, "Modeling dry matter losses from carrots during blanching", J. Food Process Eng., 9 (1987) 201–211.

[24] I., Lamberg, 'Transport phenomena in potato tissue". Ph.D. thesis, University of Lund, Lund, Sweden; (1990).

[25] G.C., Leach, DL., Pyle, K., Niranjan, 'Effective diffusivity of total solids and pectic substances from apple tissue", Int. J. Food Sci. Technol., 29 (1995) 687–897.

[26] A., Lenart, PP., Lewicki, J., Dziuda, "Changes in the diffusional properties of apple tissue during technological processing". In: Spiess WEL, Schubert H., editors. Engineering and food, vol.1: Physical properties and process control. London: Elsevier Applied Science; (1989) pp. 531-540.

[27] G., Rodger, R., Hastings, C., Cryne, J., Bailey, "Diffusion properties of salt and acetic acid into herring and their subsequent effect on the muscle tissue". J. Food Sci., 49 (1984) 714-732.

[28] P., Tomasula, MF., Kozempel, "Diffusion coefficients of glucose, potassium, and magnesium in Maine Russet Burbank and Maine Katahdin potatoes from 45 to 90°C", J. Food Sci. 54 (4) (1989) 985–999.

[29] H.G., Schwartzberg, R.Y., Chao, "Solute diffusivities in leaching process", Food Technol., 36, (1982) 73-86.

[30] D.D., Gertenbach, "Solid-liquid extraction technologies for manufacturing nutraceuticals", Shi, J., Mazza, G., Maguer, M.L., eds., Functional Foods: Biochemical and Processing Aspects (Vol.2), CRC Press, Boca Raton, Flordia (2002).

[31] J.E., Cacace, G., Mazza, "Pressurized low polarity water extraction of lignans from whole flaxseed", J. Food. Eng., 77 (2006) 1087-1095.

[32] Th., Anekpankul, M., Goto, M., Sasaki, P., Pavasant, A., Shotipruk, "Extraction of anti-cancer damnacathal from roots of *Morinda citrifolia* by subcritical water", Sep. Purif. Technol., 55 (2007) 343-349.

[33] E., Reverchon, "Mathematical modeling of supercritical extraction of sage oil," A.I.Ch.E. Journal, 42 (1996).1765-1771.

[34] Y. Jaluria, "Computer Methods for Engineering". Allyn and Bacon, Newton, MA, U.S.A. (1988).

[35] C. R. Wilke, P. Chang, "Correlation of diffusion coefficients in dilute Solutions", AICHE Journal, 1 (1955) 264-270.

[36] K. Joback, R. Reid, "Estimation of pure component properties from group contributions", Chemical Eng. Commun., 57 (1987) 233-243.

[37] C. S. Tan and D. C. Liou, "Axial dispersion of Supercritical carbon dioxide in packed beds," Ind. Eng. Chem. Res., 28 (1989) 1246-1250.

[38] J. R. Welty, C. E. Wicks, R. E. Wilson, "Fundamentals of Momentum, Heat, and Mass Transfer", 3rd ed., John Wiley & Sons, New York, (1984).

[39] R. Perry, D. W. Green, J. O. Maloney, "Perry Chemical Engineers Handbook," 5rd ed. McGraw-Hill, New York (1984).

IntechOpen

IntechOpen